Nature Environment & Pollution Technology

Modeling Landslide Hazard in the Eastern Himalayan Mountain Region of the Papumpare District of Arunachal Pradesh, India Using Multicriteria Decision-Making (MCDM) and Geospatial Techniques

Tilling Riming, Praduyt Dey†, Santanu Kumar Patnaik and Manju Narzary

Department of Geography, Rajiv Gandhi University, Itanagar, Arunachal Pradesh, India

†Corresponding author: Praduyt Dey; praduytd25@gmail.com

Manju Narzary: 0009-0000-8127-2590

Tilling Riming: 0009-0007-7368-1651

Praduyt Dey: 0009-0008-1996-0075

Santanu Kumar Patnaik: 0000-0002-6341-7319

Key Words	Analytical hierarchy process, Landslide zones, ROC curve, Landslide hazard management
DOI	https://doi.org/10.46488/NEPT.2024.v24i01.B4208 (DOI will be active only after the final publication of the paper)
Citation of the Paper	Tilling Riming, Praduyt Dey, Santanu Kumar Patnaik and Manju Narzary, 2025. Modeling Landslide Hazard in the Eastern Himalayan Mountain Region of the Papumpare District of Arunachal Pradesh, India Using Multicriteria Decision-Making (MCDM) and Geospatial Techniques. *Nature Environment and Pollution Technology*, 24(1), B4208. https://doi.org/10.46488/NEPT.2024.v24i01.B4208

ABSTRACT

Landslides are significant natural hazards that cause damage to the environment, life, and properties, mainly in hilly terrain. This research was mostly focused on generating a landslide susceptibility zone map of Papumpare District, Arunachal Pradesh, and classifying the region from high susceptibility to least susceptibility using AHP modeling techniques considering the landslide causative factors. The Analytical Hierarchy Process (AHP) is a multicriteria decision-making model (MCDM) in which each parameter is compared based on its role in triggering a landslide. A total of eight parameters were selected based on the factors that could affect the most, like Slope, Rainfall, Drainage Density, Lineament Density, Geomorphology, Soil, Geology, and Land use/Land cover. These layers were prepared using ArcGIS 10.8 software and ERDAS IMAGINE 2014. Based on the output, the region was classified into five zones of landslide susceptibility classes. Of these, the high-very-high landslides are mostly amassed near the steep and disturbed slopes due to earth-cutting, especially for building or construction of roads. Validation was done using the ROC curve (73.2%) suggesting good performance of the model. The outcome of

this work will provide information for proper landslide hazard management and will help in formulating suitable mitigation strategies in the future.

INTRODUCTION

Natural disasters are emerging as a huge threat to human life, property, and the environment. Landslides, a significant hazard, are more severe and frequent in the regions where topography is rugged and human settlements are sparse. Many natural factors such as earthquakes, heavy rainfall, river bank erosion by flood water, anthropogenic activities including development of infrastructures, deforestation, slope excavation causing slope failure, building townships in environmentally sensitive zones, etc, have also amplified the impact of disasters. Climate-induced disasters such as floods, landslides, and cyclones are increasing concerns among the community. These climate-induced disasters are projected to become more severe with region-specific intensification (IPCC 2021). Landslides serve as one of the most catastrophic geological hazards in the hilly regions. It is more frequent in high mountainous regions where cloudburst-induced extreme rainfall causes huge movement of debris down the slope (Kirschbaum et al. 2020). In recent years, landslide events have modified landforms, affected biodiversity, triggered various hazards like floods, earth-cutting, and alteration of river courses due to sedimentation, and damaged life and properties (Lombardo et al. 2020, Hao et al. 2023).

India's distinct climate and geodynamics make it susceptible to various naturally occurring disasters. Studies show that about 60% of its landmass is susceptible to earthquakes of different magnitudes, about 8% to cyclone hazards, about 68% to drought, 12% to floods, and approximately 15% area is vulnerable to landslides. Nearly 14% of India’s land area is landslide-prone, among which one-fifth falls under the northeastern region (Raju 2002). Almost the entire NE region is susceptible to landslides of various degrees due to its complex terrain conditions.

Landslide zonation maps formulated through geospatial technologies are crucial in disaster management and risk mitigation (Kanwal et al. 2016, Huan et al. 2023). According to Fell et al. (2007, 2008) and AGS (2000), landslide hazard zonation means the classification of terrain into different zones that are characterized based on the spatial and temporal probability of the phenomenon, including location, volume, and future prediction of landslide occurrence. The availability of high-resolution spatial data, geoinformatics, and fast-processing computers has automated landslide hazard/susceptibility mapping processes, minimizing fieldwork and delineating potential landslide-affected areas (Ilanloo 2011). In recent years, several techniques have been utilized for the identification and assessment of landslide susceptibility zones, including machine learning (ML) (Jhunjhunwalla et al. 2019, Merghadi et al. 2020), logistic regression model (Hemasinghe et al. 2018, Shano et al. 2022), analytical hierarchy

process (Das et al. 2022, Barman et al. 2024), frequency ratio (Yadav et al. 2023, Qazi et al. 2023). Many researchers have experimented with GIS using various causative factors to perform models for landslide hazards (Sarkar & Kanungo 2004, Hong et al. 2007, Kouli et al. 2010, Avtar et al. 2011, Othman et al. 2012, Devkota et al. 2013, Paulín et al. 2014, Ahmed 2015, Pareta & Pareta 2015, Younes Cárdenas and Mera 2016, Hadmoko et al. 2017, Stanley & Kirschbaum 2017, Mahdadi et al. 2018). This requires the identification of those areas that are or could be affected by landslides and the calibration of the chances of such landslides occurring within a specific period. Commenting on the eventuality of landslides through zonation mapping itself is a challenging task. The LHZ maps do not directly incorporate the magnitude and time before or after the occurrences. The methodology to develop a susceptibility map hinge on several elements, viz., the nature of the terrain, parameters to be considered, available data on slope, rainfall, seismicity, geology, soil, etc. The AHP techniques are very productive in identifying potential landslide zones as they depend on subjective knowledge and expert judgments and are constantly checked through consistency measures (Veerappan et al. 2017, Ozioko & Igwe 2020). Thus, for minimizing the impact of landslides, the AHP-based susceptibility map becomes important since the area is classed between very low hazard to very high hazard zones based on different landslide hazard zones (Arora et al. 2004). Landslide hazard mapping offers knowledge that helps designers and engineers locate landslide-prone areas to implement effective mitigation measures.

Here in this study, the method used for preparing the zonation map of the Papumpare district is the GIS-based-Analytical Hierarchy Process (AHP), given by (Saaty 1980). AHP is an accepted multicriteria decision-making analysis method that has been widely applied to many decision-making systems. AHP technique integrated with the landslide hazard map makes it more reliable (Feizizadeh et al. 2014). This research attempts to produce information that can be useful for predicting the location of future landslides in the Papumpare district of Arunachal Pradesh which will help the planners and policymakers in the effective management of landslide hazards in the region.

STUDY AREA

The Papumpare district is situated in the southwestern part of Arunachal Pradesh, bordering Assam. The name Papumpare is procured from the rivers Papum and Pare, which flow through the district. Papumpare district lies between 93°12' E to 94°13' E Longitudes and 26°56' N to 27°35' N Latitudes (Fig. 1). The district covers a geographical area of 3462 sq.km in the lesser Himalayan zone. It is bounded by Lower Subansiri and Kurung Kumey districts in the north, East Kameng district in the west, and North Lakhimpur district of Assam in the east

and south. Papumpare ranked 14th among the districts of Arunachal Pradesh in terms of area. The district is covered by thick forest which has sub-tropical, deciduous, and humid types of vegetation. Mostly, the low-lying regions and valleys are occupied by inhabitants. The Hill range approximately varies from 300 m to 2700 m above sea level. Itanagar, the state capital, is situated at an altitude of 440m above MSL.

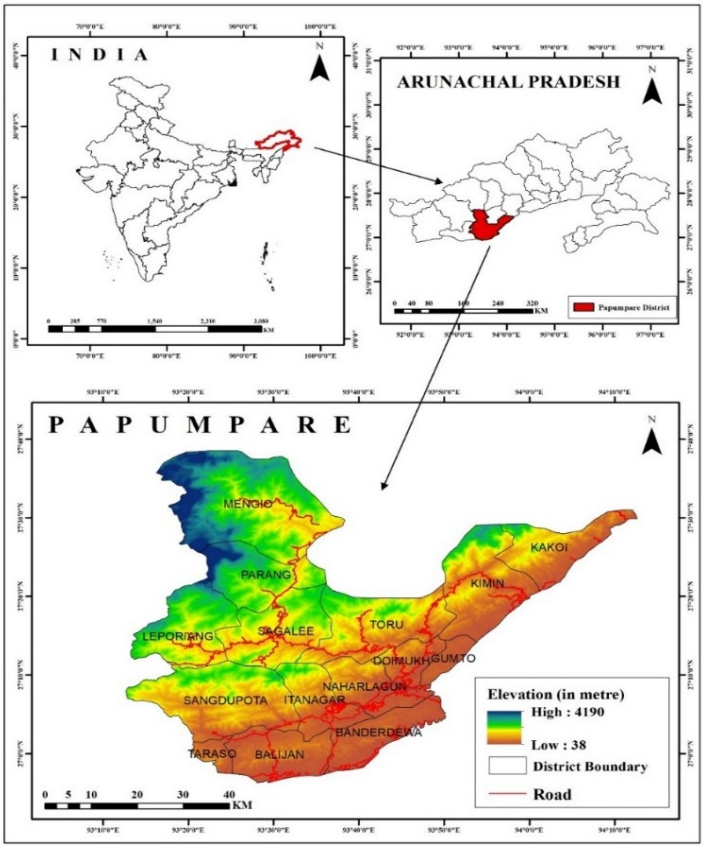

Fig. 1: Locational Map of the Papum Pare District, Arunachal Pradesh.

MATERIALS AND METHODS

Data Sources

Several causative factors which are responsible for landslides were studied for this project. The study is solely based on the secondary data obtained from various sources (Table 1). The selected factors were slope, rainfall, drainage density, lineament density, geomorphology, soil type, geology, and land use/land cover. Various thematic layers were generated within ArcGIS software 10.8 to develop the LSZ map. A topographical map of scale 1:50,000 from the Survey of India has been georeferenced. Cartosat-3, version 3 (1.12 m resolution) DEM was employed to develop slope and drainage density maps. For rainfall, the data were downloaded from the Climate

Hazards Group InfraRed Precipitation with station data (CHIRPS 0.05° resolution). The spatial distribution of rainfall data for the study is estimated using the interpolation method (Kriging). LULC map was generated from Landsat-8 OLI by supervised classification in ERDAS IMAGINE 2014. The Geomorphology, Geology, and Lineament map of the study area was obtained from the Geological Survey of India. Soil data were collected from the Food and Agriculture Organization (FAO).

Table 1: Database and its sources.

Data	Source
Cartosat-3, version 3 (1.12m resolution) DEM	Downloaded from NRSC-Bhuvan, https://bhuvan-app1.nrsc.gov.in/
CHIRPS Annual Rainfall data (0.05° resolution)	Downloaded from Climate Hazard Centre, UC Santa Barbara, https://data.chc.ucsb.edu/products/CHIRPS-2.0/
LULC from satellite image Landsat-8 OLI	Downloaded from the United States Geological Survey, http://earthexplorer.usgs.gov/
Lineament, Geology, Geomorphology	Downloaded from Geological Survey of India, https://bhukosh.gsi.gov.in/
Soil data	Downloaded from the Food and Agriculture Organization of the United Nations (FAO), https://www.fao.org/

Application of AHP Techniques

The AHP (Saaty 1980) is a technique employed to determine the weight of different parameters. Relative ratings/scores were assigned to every parameter according to the level of influence, the literature review, and expert opinions. Each class of parameter was graded using Saaty's nine-point weighing scale (0-9), i.e., the pairwise comparison matrix (Table 2), where a high rating indicates a high influence on the occurrence of landslides. The final layout for the LHZ map was carried out by using weighted overlay analysis within the ArcGIS 10.8 software using each of the generated thematic layers.

According to Gorsevski et al. (2006), AHP is a hierarchical structure of a pairwise comparison matrix consisting of equal rows and columns. For formulating a comparison matrix, each parameter is rated against each one of the parameters by assigning a rate that is relatively more dominant. The scale ranges between 1 to 9 (Table 2). Thus,

comparison matrices are pursued as input, and the relative weights are accorded as output. Fig. 2 shows the methodological framework adopted in delineating the landslide inventory map of Papumpare district, Arunachal Pradesh.

Table 2: Weights for Pairwise comparison. Source: (Saaty 1990).

Scales	Intensity	Descriptions
1	Equally important	Both factors are important
3	Slightly important	One among others is slightly more effective than a certain factor
5	Quite important	One among others strongly tends to a certain factor
7	Extremely important	One among others is extremely dominant to a certain factor
9	Absolutely important	A factor has the highest possibility of tending to a certain factor

Computation of the Weights Assigned to Parameters

After assigning the pairwise comparison matrix (Table 3), the calculation was done. The comparison matrix in AHP consists of rows and columns; each row of the matrix is compared to the other, and each row indicates the relative significance between the two criteria. In this matrix, the rows follow the inverse of each criterion and its significance with others (Bera et al. 2019). Subsequently, the weights were normalized (Table 4) to minimize the biases that exist in the weight assignment (Saravanan et al. 2021).

The calculation of the Consistency ratio (CR) validates the result and was coined to consider whether the comparison matrix is consistent or not (Kolat et al. 2012).

$$\text{Consistency Ratio (CR)} = \frac{\text{CI}}{\text{RI}}$$

$$\text{CI} = \frac{\lambda\text{max} - \text{n}}{\text{n} - 1}$$

Where λ - eigenvalue and n - number of factors.

To determine the Consistency Index, AHP compares it by Random index (RI), and the result is called Consistency Ratio, which can be defined as CR = CI/RI. The Random index (Table 5) is the randomly generated comparison matrix of order 1 to 10 obtained by approximating random indices (Saaty 1990). Table 3 shows the value of RI.

As per the values of CR, if CR is less than 0.10, the ratio indicates a sensible level of consistency for the given pairwise comparisons. Thus, if CR is greater than 0.10, then the ratio indicates inconsistent judgments. In certain cases, the assigned values for the given matrix should be reconsidered and re-evaluated.

Based on this study, the calculated overall value for the consistency ratio was 0.065, which shows that the comparisons of each factor/parameter indicate a reasonable consistency and that the weights (Table 6) were appropriate for the model.

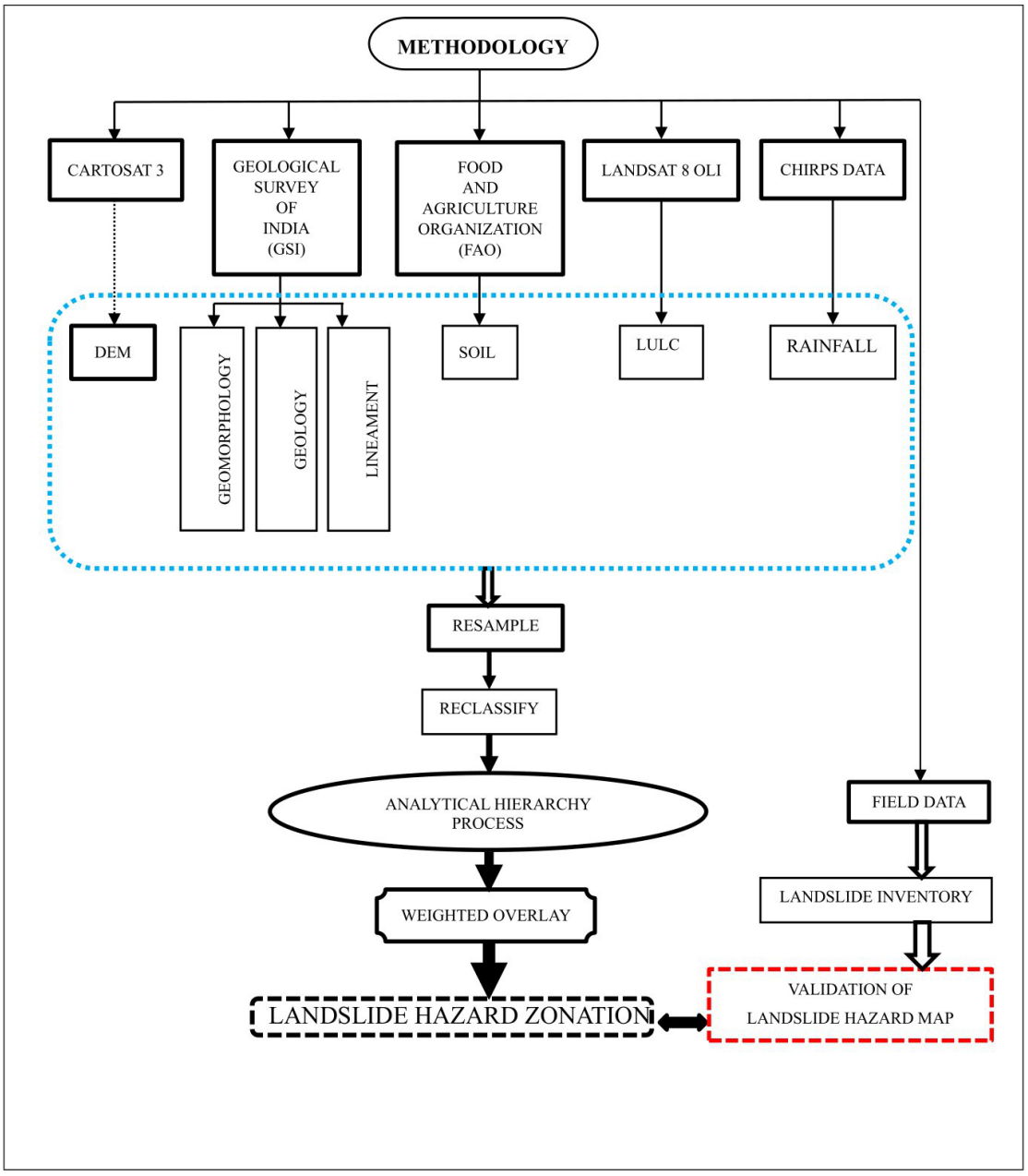

Fig. 2: Conceptual Framework.

Table 3: Pair-wise comparison matrix.

CRITERIA	SL	RF	DD	LD	GE	SO	G	LULC
Slope (SL)	1	2	3	3	4	5	6	7
Rainfall (RF)	0.5	1	2	4	5	5	6	7
Drainage density (DD)	0.33	0.5	1	2	3	4	6	6
Lineament density (LD)	0.33	0.25	0.5	1	3	4	6	6
Geomorphology	0.25	0.2	0.33	0.33	1	2	3	5
Soil	0.2	0.2	0.25	0.25	0.5	1	3	4
Geology (G)	0.17	0.17	0.17	0.17	0.33	0.33	1	3
LULC	0.14	0.14	0.17	0.17	0.2	0.25	0.33	1

Table 4: Standardized comparison matrix and calculation of criterion weights.

CRITERIA	SL	RF	DD	LD	GE	SO	G	LULC	Total Weight	Standardized Weight
Slope (SL)	0.34	0.45	0.40	0.27	0.23	0.23	0.19	0.18	2.31	0.29
Rainfall (RF)	0.17	0.22	0.27	0.37	0.29	0.23	0.19	0.18	1.93	0.24
Drainage density (DD)	0.11	0.11	0.13	0.18	0.18	0.19	0.19	0.15	1.25	0.16
Lineament density (LD)	0.11	0.06	0.07	0.09	0.18	0.19	0.19	0.15	1.03	0.13
Geomorphology	0.09	0.04	0.04	0.03	0.06	0.09	0.10	0.13	0.58	0.07
Soil	0.07	0.04	0.03	0.02	0.03	0.05	0.10	0.10	0.44	0.06
Geology (G)	0.06	0.04	0.02	0.02	0.02	0.02	0.03	0.08	0.28	0.03
LULC	0.05	0.03	0.02	0.02	0.01	0.01	0.01	0.03	0.18	0.02

Table 5: Random Index.

N	1	2	3	4	5	6	7	8	9	10
RI	0.0	0.0	0.58	0.90	1.12	1.24	1.32	1.41	1.45	1.49

Table 6: Consistency Vector for each criterion.

CRITERIA	Weight	Consistency Vector
Slope	2.56	8.87

Rainfall	2.22	9.20
Drainage	1.41	9.03
Lineament	1.14	8.84
Geomorphology	0.61	8.45
Soil Type	0.46	8.32
Geology	0.28	8.10
LULC	0.18	8.33

Eigenvector λ = sum of consistency vector/ no. of parameters(N)

$\lambda = 8.64$

Consistency Index = 0.092

Consistency Ratio = 0.065

RESULTS AND DISCUSSION

Slope

The slope plays a major role, as the degree of slope angle is considered the main causative factor used to generate the susceptibility in landslides. According to (Lee et al. 2004), as the degree of slope angle increases, shear stress in soil or overlying material increases as well. The slopes of the study area (Fig. 3) were classified into five categories such as steep (>50°), which cover 301.49 sq. km, and high (31°- 40°) covers 798.41 sq. km. Moderately high (21°- 30°) covers 1024.26 sq. km, gentle (11°- 20°) covers 897.96 sq. km, and rolling slopes (<10) which covers 497.57 sq. km. A steep slope with more mobilizing force may fail early (Anbalagan et al. 2015). In steeper slopes, due to gravity, the weight of the underlying material will be more compared to moderate slope, thus, the weights were allotted accordingly (Table 7).

Rainfall

Landslides triggered by rainfall are primarily caused by the build-up of pore water pressures in the ground (Sengupta et al. 2010). For the preparation of the rainfall distribution map (Fig. 4), 10-year rainfall data were considered. The intensity of the annual average rainfall of the region ranges between 864 and 2884 mm. The rainfall map was divided into five categories, namely, 864-1268 mm, which covers 465.47 sq. km, 1268-1664 mm

covers 708.40 sq. km, 1664-2012 mm covers 987.89 sq. km, 2012-2392 sq. km, and 2392-2884 mm which covers 591.84 sq. km. Higher intensity of rainfall was found in the eastern part of the region, and the northern region showed moderate-intensity rainfall (864-1664 mm). Intense rainfall during monsoon causes rainwater seepage, due to which the materials get saturated and loosened, this, in turn, causes slope failure. Higher rainfall zones were provided with high weights and vice-versa (Table 7).

Drainage Density

Drainage is an important factor that controls the landslide as its densities control the nature of the soil and its geotechnical properties (Pareta 2004). The function of infiltration is negatively correlated to drainage density. High-density values are indicative of lower infiltration rates and higher surface flow velocity. The lower the infiltration rate, the more favorable it is for runoff, thus indicating higher drainage density. The study area (Fig. 5) has been divided into five classes, namely, 0.01-0.22 km/sq.km, which covers a 438.62 sq.km area, 0.22-0.34 km/sq.km covers 828.2 sq.km, 0.34-0.44 km/sq.km covers 939.57 sq.km, 0.44-0.55 km/sq.km covers 818.31 sq.km and 0.55-0.78 km/sq.km covers 505.3 sq.km. High-density values, i.e., between 0.01- 0.78 km/sq.km, are witnessed in whole parts of the region. The susceptibility of landslide zones is proportional to the function of drainage density due to its relation with surface runoff and permeability. The weights were allotted according to the dominance of drainage in different locations of the Papumpare district (Table 7).

Lineament Density

Lineament is a linear feature in a landscape that is an expression of an underlying geological structure, such as a fault. Lineament appears as a fault-aligned valley, fold-aligned hills, straight coastline, or union of these features. Lineament helps to surmise mineral prospects of a region, analyze structural deformation patterns/trends, identify geological boundaries, and surmise crustal structure and various subsurface phenomena in areas of unexposed lithology. Lineament and any planar structure are important factors for assessing the stability of slopes which destabilize the area as well as lead to the deterioration of rocks, which energize the weathering processes. The lineament density varies between 0 and 74.9 km/km square. Hence, the Lineament density (Fig. 6) has been classified upon natural breaks into 5 classes such as class I (0-6.46 km/sq.km), class II (6.46-18.21 km/sq.km), class III (18.21-31.42 km/sq.km), class IV (31.42-42.04 km/sq.km), class V (49.04-74.9 km/sq.km). The regions with high lineament density values were provided with higher weights and vice-versa (Table 7).

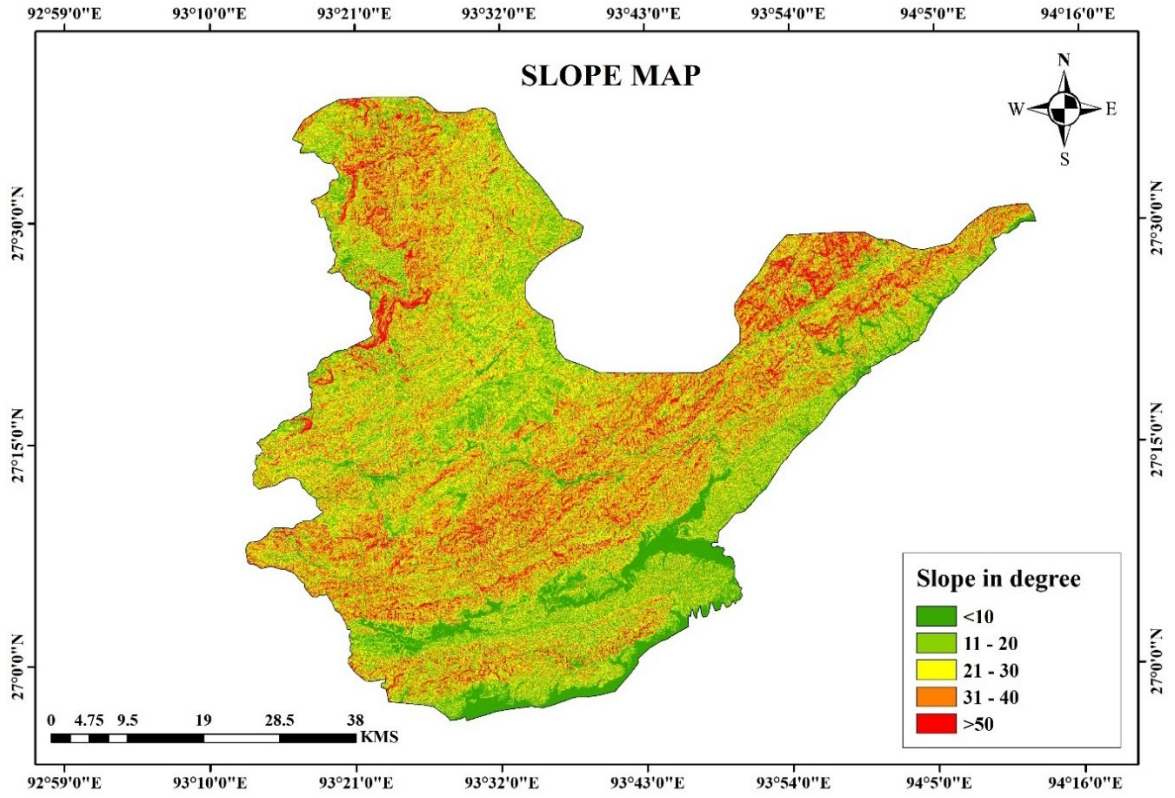

Fig. 3: Slope map.

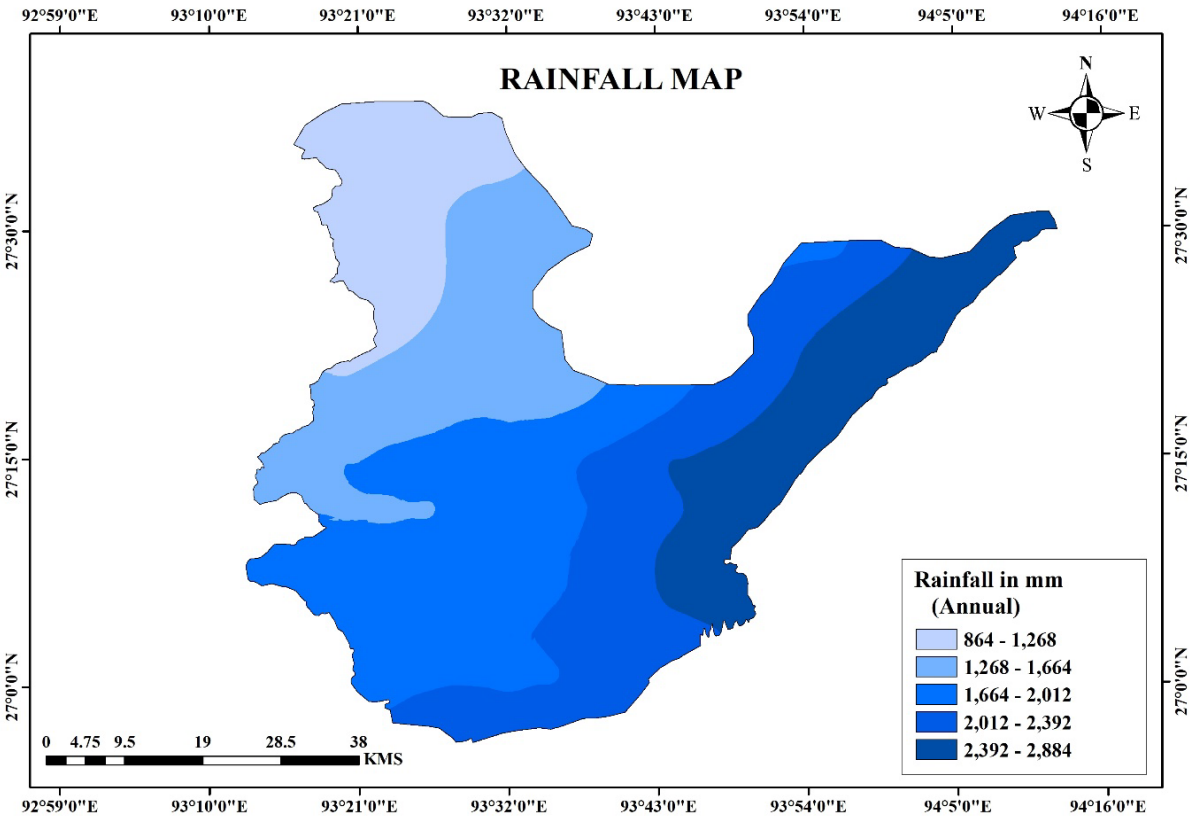

Fig. 4: Rainfall map.

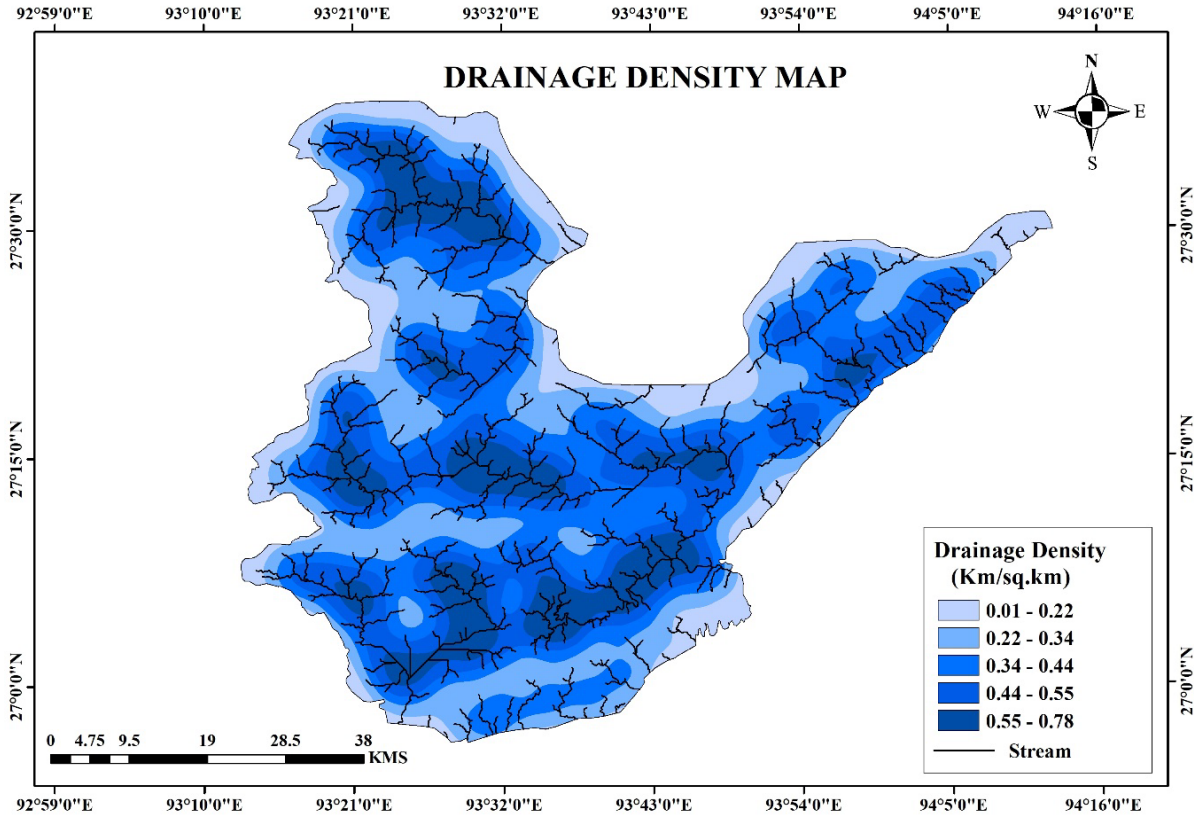

Fig. 5: Drainage Density map.

Geomorphology

The geomorphologic map depicts important geomorphic units, landforms, and underlying geology to provide an understanding of the processes, lithology, structures, and geologic controls related to landslide susceptibility. The geomorphology of the region (Fig. 7) consists of a river, an alluvial/flood plain, highly/low dissected structural hills, a pediment/piedmont slope, and mass wasting. The region is mostly mountainous, forming a part of the eastern Himalayan ranges. The high/low dissected structural hills dominate the region with 3361.44 sq. km of areal coverage comprising 95.23% of the geographical area of the region, followed by alluvial/flood plain with 96.60 sq.km (2.73%), rivers occupying 49.83 sq.km (1.41%), pediment slope covering 21.53 sq.km (0.60%) and the rest are mass wasting products spread across 2.33 sq.km area (0.06%). The weights are ranks assigned to the geomorphological class, and sub-classes are depicted in Table 7.

Soil

Soil texture, soil depth, and soil erosion play an important role in assessing the stability of the soil and landslide susceptibility of the land. In the case of soil texture, the landslide occurrence probability value is higher in rocky and sandy loam and is lower in fine sandy loam, silt/gravelly silt loam, and loam (Lee et al. 2004). According to

the generated soil map (Fig. 8), the region is mainly composed of three soil types: loamy soil (1516.33 sq.km areal coverage), fine loamy soil (1054.44 sq.km), and coarse loamy soil (959.18 sq.km). The study shows that lightweight soils like sandy and coarse loams are easy to detach as they need low organic matter content, leading to an inability to stable aggregates. Therefore, soil with a lot of sand, steep slopes, and intensive fall, which represent the most dominant factors of landslide, cause severe harm to the land, and thus, weights were provided accordingly (Table 7). Thus, the susceptibility of an area to landslide increases with the increase of soil erosion.

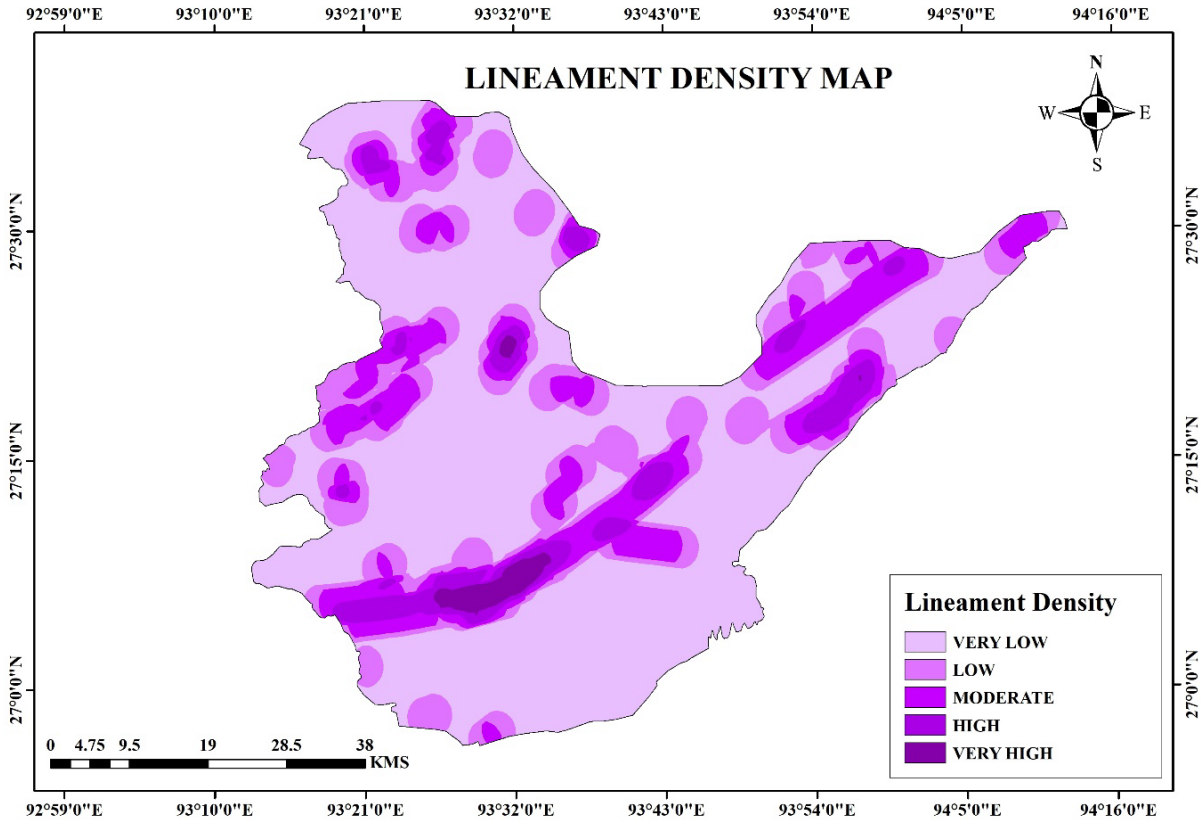

Fig. 6: Lineament Density map.

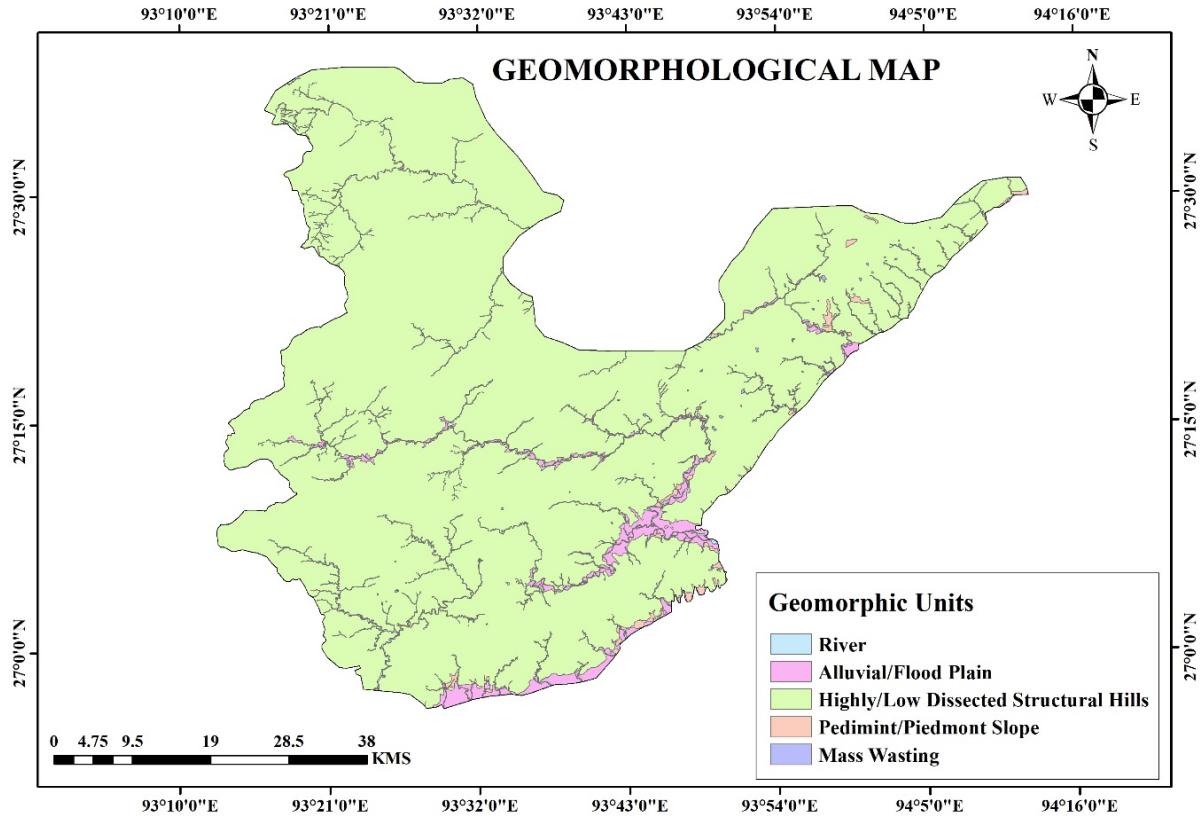

Fig. 7: Geomorphology.

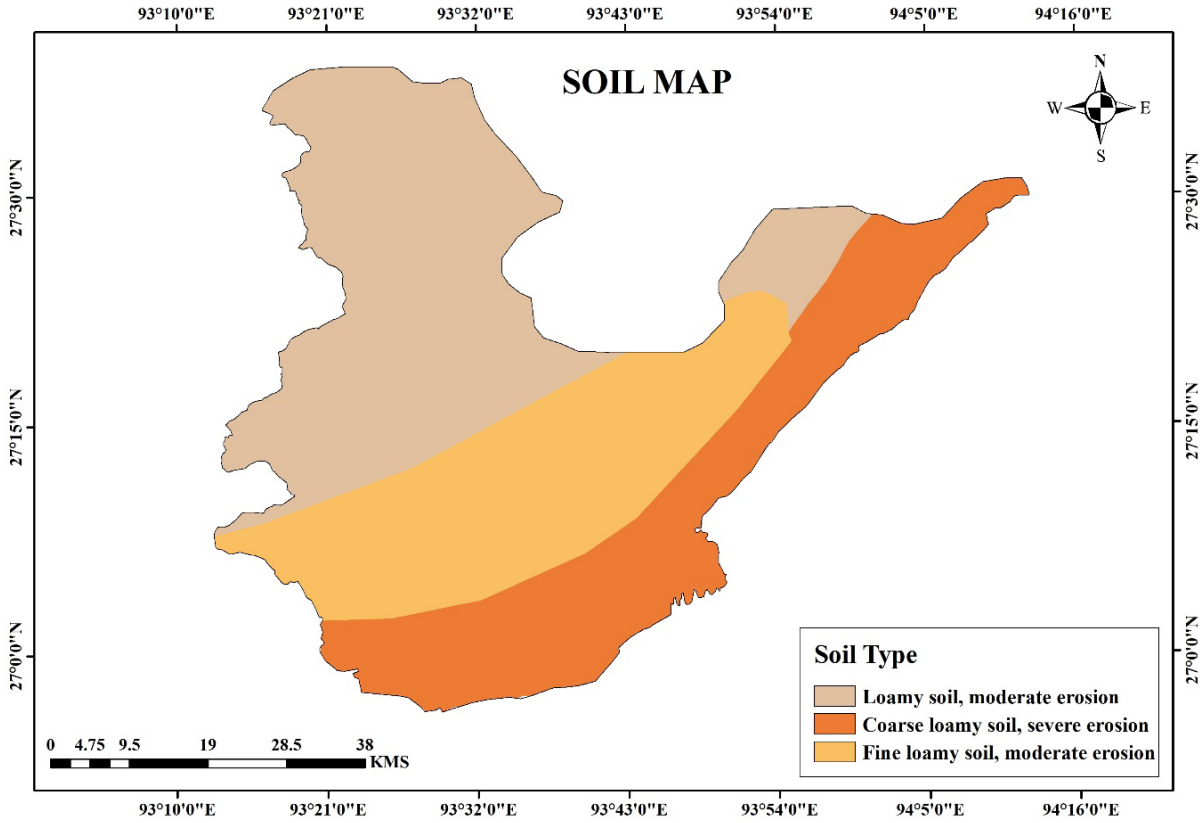

Fig. 8: Soil map.

Geology

Lithology is one such factor that is oftentimes used for landslide susceptibility analysis in the hilly area (Althuwaynee et al. 2016). Landslides generally depend on the rock properties of the region because of the variance in strength and permeability of rocks. Due to heavy rainfall, weak or highly weathered or eroded rocks cause frequent landslides in different places around the world. In the study area (Fig. 9), the rocks that are the most dominant are the Siwalik group (59.28% area), followed by Undifferentiated Quaternary sediments (39.22% area), the Bomdila group (1.14% area) and the Lower Gondwana group (0.34% area). The region dominated by undifferentiated quaternary sediments was assigned the highest weight due to its unstable structure, and the Bomdila group was given the least weight as these rocks are comparatively older and more stable (Table 7).

Land-use/Land-cover

Alteration in land use/land cover is a crucial factor for landslide susceptibility models. Anthropogenic factors like the construction of buildings, roads, bridges, deforestation, etc., in the hilly regions also contribute to the event of landslides due to the instability of the slope. The LULC map (Fig 10) was prepared using Landsat 8 OLI satellite data. Five categories of land use/land cover were classified in the region, namely, dense forest (3385.23 sq.km), cropland (30.72 sq.km), sandbar (5.78 sq.km), rivers (10.02 sq.km), and settlement (98.25 sq.km) were identified. In general, the region has a dense vegetation cover with thick evergreen forests, which are very less susceptible to landslides and, thus, were assigned the lowest weight. The weights assigned to each LULC sub-class are depicted in Table 7.

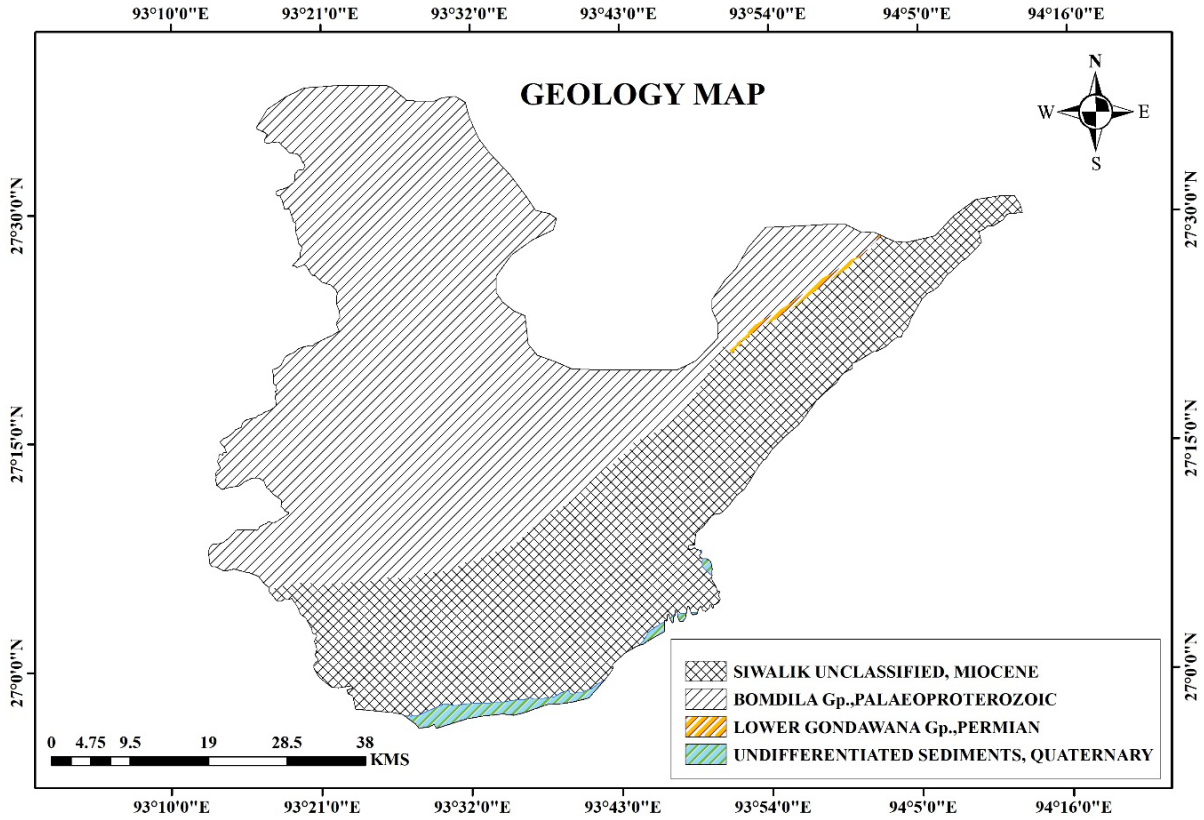

Fig. 9: Geology.

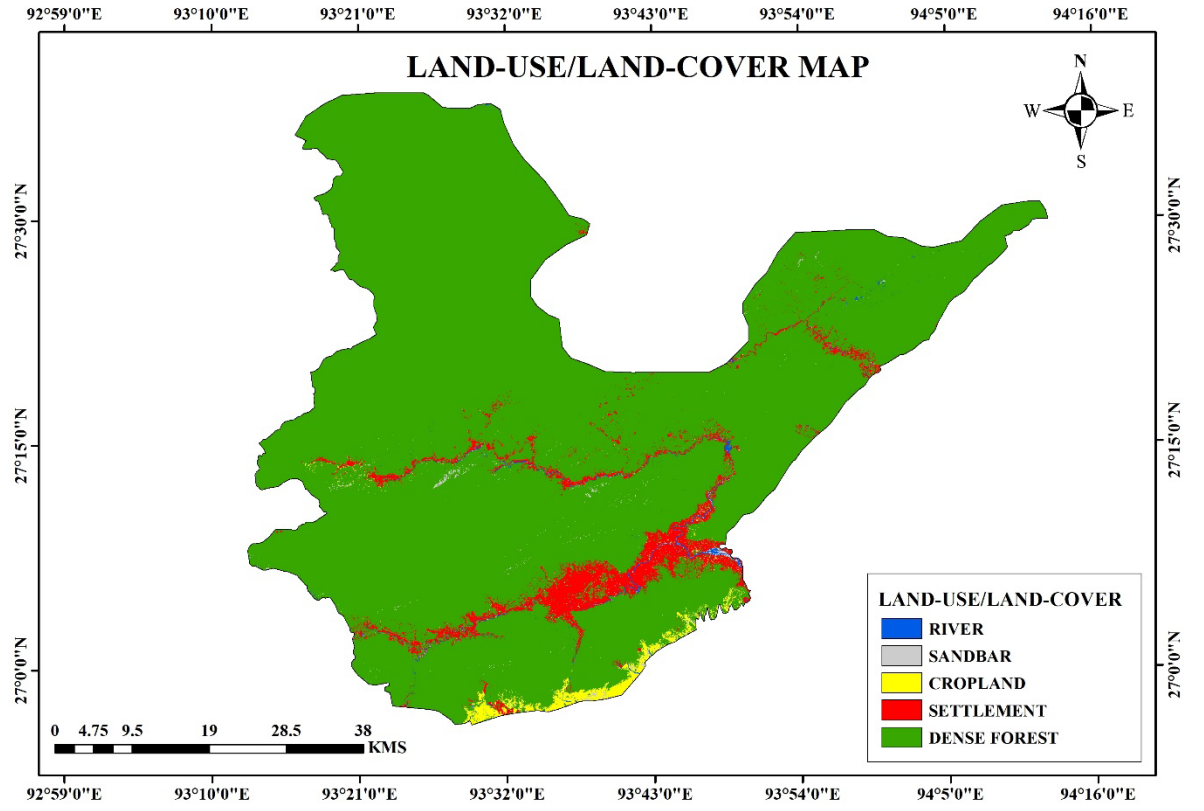

Fig. 10: Land use/Land cover map.

Landslide Hazard Zonation

The LSZ map was delineated by weighted overlay analysis which was performed in ArcGIS 10.8 software, with reference to the eight parameters cited above. The weighted values of each parameter (Table 7) indicate the impact of each parameter on another. Accordingly, the susceptibility map of the region contains five zones, based on the landslide susceptibility index such as "very low hazard, low hazard, moderate hazard, high hazard, and very high hazard" (Fig. 11). Table 8 signifies that 6.35% (223.55 sq. km) of the area falls under the very high zone, 26.29% (925.02 sq. km) has a high zone, 40.68% (1431.43 sq. km) in the moderate zone, 26.69% (938.24 sq. km) in low zone and only 0.003% (0.12 sq. km) has a very low potential for the occurrence of landslide. Most of the area falls under the moderate to high zone. The map demonstrates that the high to very high-landslide-hazard zone was concentrated in the following circles, i.e., Doimukh, Itanagar, Kakoi, Kimin, Naharlagun, Sangdupota, Toru, etc. Most of the concentrated hazard zones are seen near steep terrains and disturbed slopes because of earth-cutting for the construction of roads, buildings, etc. Areas that have low-hazard potential zones are largely concentrated in the southern part of the district, which are mostly low-lying regions. The delineated zonation map shows that the degree of landslide hazard decreases with increasing distance from drainage, lineament, and settlements.

Table 7: Landslide hazard weights values and rating system of different thematic layers.

Factors	Classes	Weights	Rating	Consistency Ratio
Slope (in degree)	<10 11-20 21-30 31-40 >50	0.29	1 3 5 7 9	0.017
Rainfall (in mm)	864-1268 1268-1664 1664-2012 2012-2392 2392-2884	0.24	5 6 7 8 9	0.045
Drainage Density [Km.sq.km^{-1}]	0.01-0.22 0.22-0.34 0.34-0.44 0.44-0.55 0.55-0.78	0.16	1 3 5 7 9	0.016

Lineament Density [Km.sq.km^{-1}]	0-6.46 6.46-18.21 18.21-31.42 31.42-42.04 49.04-74.9	0.13	1 3 5 7 9	0.020
Geomorphology	River Alluvial/Floodplain Highly/low dissected structural hills Pedimont/Piedmont slope Mass Wasting	0.07	3 4 5 6 7	0.039
Soil	Loamy soil, moderate erosion Fine loamy soil, moderate erosion Coarse loamy soil, severe erosion	0.06	4 5 6	0.006
Geology	Siwalik unclassified, Miocene Bomdila Gp. Paleoproterozoic Lower Gondwana Gp. Permian Undifferentiated sediment, Quaternary	0.03	6 4 5 7	0.086
LULC	River Sandbar Cropland Settlement Dense Forest	0.02	8 7 6 5 4	0.053

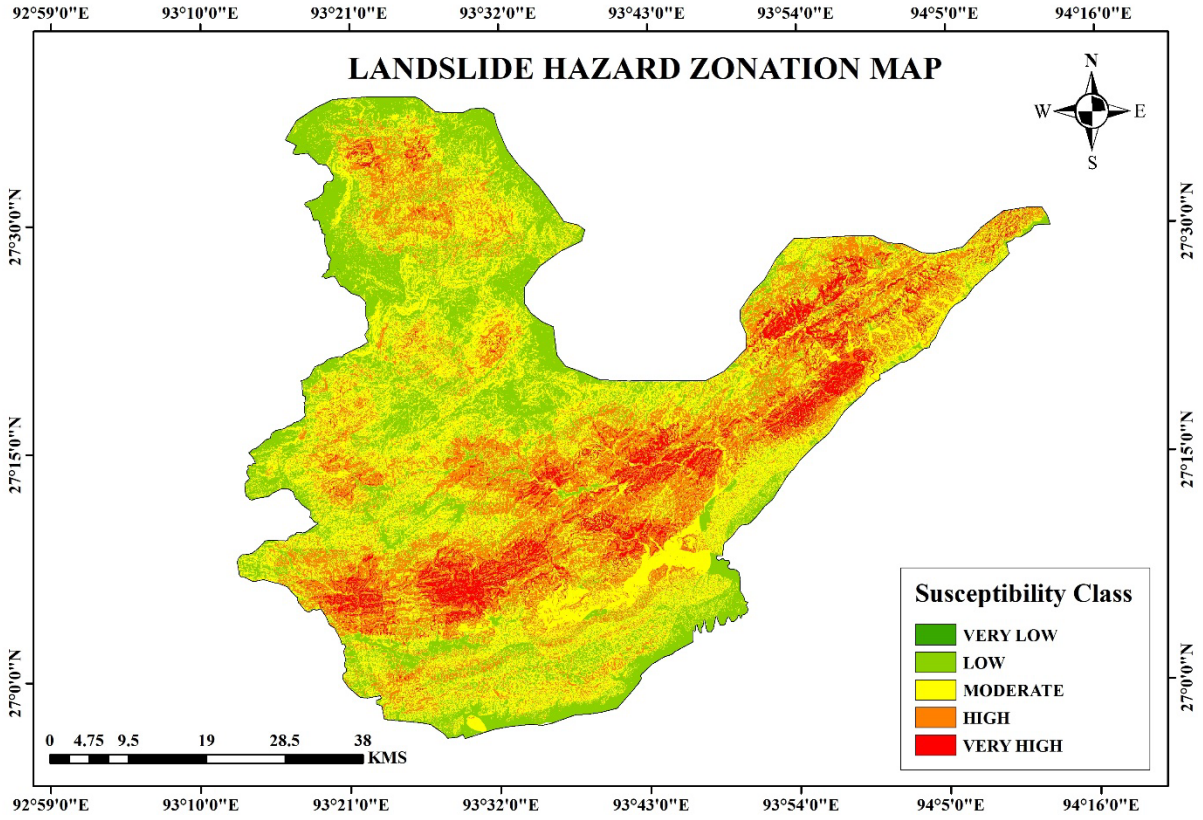

Fig. 11: LHZ map of the study area.

Table 8: Area of zones (Percentage).

Susceptibility zone	Area [km^2]	Area in Percentage [%]
Very Low zone	0.12	0.003
Low zone	938.24	26.69
Moderate zone	1431.43	40.68
High zone	925.02	26.29
Very High zone	223.55	6.35

Map Validation of LHZ Map with Field Data

Validation of the hazard zones is essential to confirm the precision rate of the landslide susceptibility map acquired based on the AHP model. In the current study, validation is done by using ROC (Receiver Operating Characteristic) as a tool for appraising the efficiency of landslide zonation. ROC curve is mostly used to show the correlation between True Positive Rate and False Positive Rate graphically (Althouse 2016). A landslide inventory map (Fig. 12) was prepared based on data collected from the Geological Survey of India and field visits. A total of hundred landslide location points were collected using the GPS device during the field survey and Geological

Survey of India and were analyzed with the LHZ map using ArcSDM tools. The value of the accuracy curve for the Area Under Curve (AUC) ranges between 0.5 to 1, and the prediction model based on the ROC curve and AHP generated a value of 0.73 or 73%, which quantifies that the prediction is good (Fig. 13). Fig. 14 shows images from the field visit identifying some active landslide zones in the Papumpare districts.

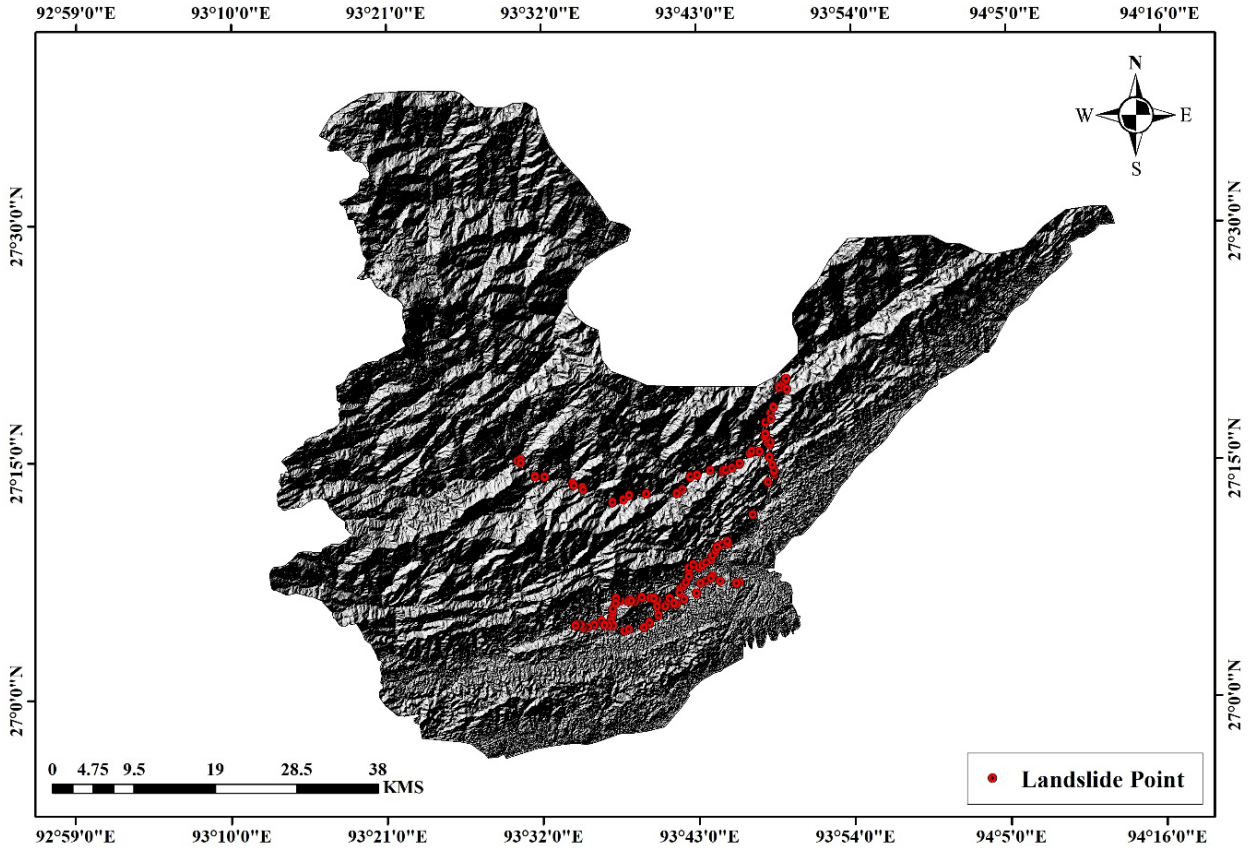

Fig. 12: Landslide inventory map.

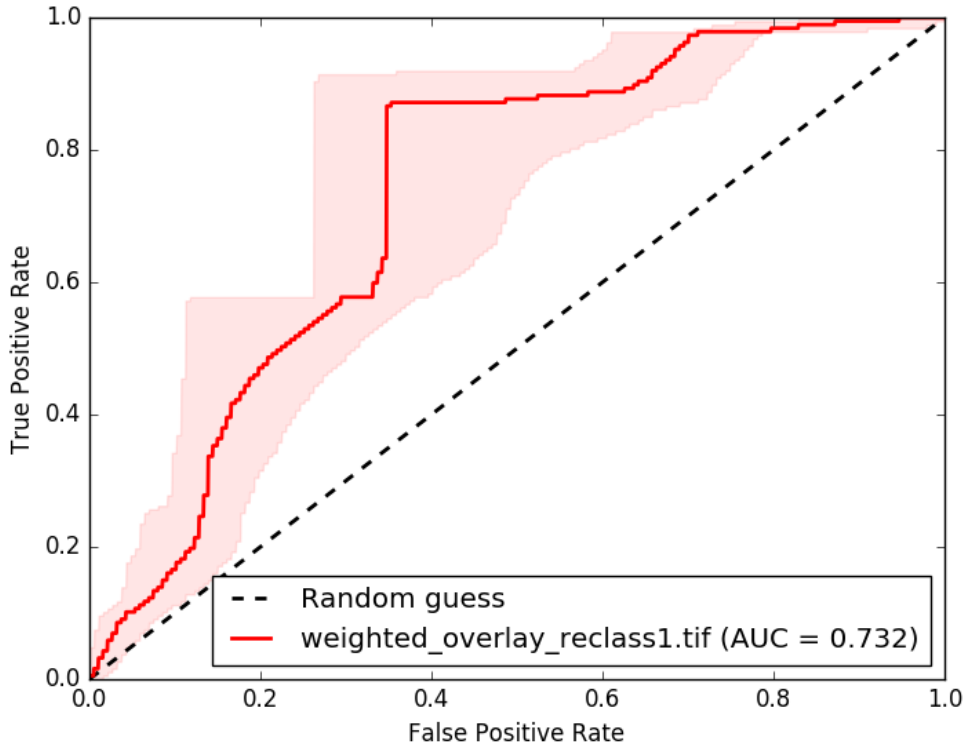

Fig. 13: ROC curve for Landslide zonation map derived from AHP.

Fig. 14: Photographs of some selected landslide sites of the study area.

Limitations and Suggestions for Future Research

The landslide hazard zonation (LSZ) of the Papumpare district using GIS and AHP techniques provided significant results. However, the research has several limitations that should be acknowledged for building a base for future studies in the region. Some of the limitations include a lack of adequate landslide data, inaccessibility due to rugged terrain conditions and limited field validation, subjectivity in the AHP model, and lack of monitoring temporal change in different landslide triggering factors. Thus, future courses of research need to be guided by the integration of real-time data, consideration of other hazards associated with landslides, and the use of GIS-based machine learning (ML) and deep learning (DL) in landslide zone mapping.

CONCLUSIONS

Papumpare, the capital district of Arunachal Pradesh, is prone to frequent landslide, which occurs every year mostly due to heavy downpours, seismic activity, and anthropogenic interference. During the monsoon season, the region faces difficulties caused by landslides, resulting in several issues like loss of life, damage of properties, and hindering social and economic progress. In the present research, potential landslide sites were identified by integrating AHP and geospatial technologies using eight landslide-triggering factors. The findings revealed that more than 70% (2,580 sq. km) of the region falls under moderate to very high landslide zones, and the rest of the region falls under low to very low landslide potential zones. The higher landslide susceptibility was witnessed in the areas affected by human intervention, higher rainfall, and geological vulnerability. The validation of the LSZ map was realized through field surveys and by generating a landslide inventory map and ROC-AUC curve with an accepted value of 0.73. The results suggest good landslide predictability. However, the improvement of the prediction accuracy of the delineated map can be further reformed by considering more factors. The resulting LHZ map of the Papumpare district can be a reliable repository of information supporting land-use planning and management of the terrain, helping to minimize the impact of landslides in the region.

REFERENCES

Ahmed, B., 2015. Landslide susceptibility mapping using multi-criteria evaluation techniques in Chittagong Metropolitan Area, Bangladesh. *Landslides*, 12, pp.1077–1095. https://doi.org/10.1007/s10346-014-0521-x

Althouse, A.D., 2016. Statistical graphics in action: Making better sense of the ROC curve. *International Journal of Cardiology*, 215, pp.9-10. http://dx.doi.org/10.1016/j.ijcard.2016.04.026

Althuwaynee, O.F., Pradhan, B. and Lee, S., 2016. A novel integrated model for assessing landslide susceptibility mapping using CHAID and AHP pair-wise comparison. *International Journal of Remote Sensing*, 37(5), pp.1190-1209. https://doi.org/10.1080/01431161.2016.1148282

Anbalagan, R., Kumar, R., Lakshmanan, K., Parida, S. and Neethu, S., 2015. Landslide hazard zonation mapping using frequency ratio and fuzzy logic approach: a case study of Lachung Valley, Sikkim. *Geoenvironmental Disasters*, 2(6), pp.1–17. https://doi.org/10.1186/s40677-014-0009-y

Arora, M.K., Das Gupta, A.S. and Gupta, R.P., 2004. An artificial neural network approach for landslide hazard zonation in the Bhagirathi (Ganga) Valley, Himalayas. *International Journal of Remote Sensing*, 25(3), pp.559–572. https://doi.org/10.1080/0143116031000156819

Australian Geomechanics Society (AGS), 2000. Landslide risk management concepts and guidelines. *Australian Geomechanics*, 35, pp.49–92.

Avtar, R., Singh, C.K., Singh, G., Verma, R.L., Mukherjee, S. and Sawada, H., 2011. Landslide susceptibility zonation study using remote sensing and GIS technology in the Ken-Betwa River Link area, India. *Bulletin of Engineering Geology and the Environment*, 70(4), pp.595–606. https://doi.org/10.1007/s10064-011-0368-5

Barman, J., Biswas, B. and Rao, K.S., 2024. Hybrid integration of analytical hierarchy process (AHP) and the multiobjective optimization on the basis of ratio analysis (MOORA) for landslide susceptibility zonation of Aizawl, India. *Natural Hazards*, 120, pp.8571–8596. https://doi.org/10.1007/s11069-024-06538-9

Bera, A., Mukhopadhyay, B.P. and Das, D., 2019. Landslide hazard zonation mapping using multi-criteria analysis with the help of GIS techniques: a case study from Eastern Himalayas, Namchi, South Sikkim. *Natural Hazards*, 96, pp.935–959. https://doi.org/10.1007/s11069-019-03580-w

Das, S., Sarkar, S. and Kanungo, D.P., 2022. GIS-based landslide susceptibility zonation mapping using the analytic hierarchy process (AHP) method in parts of Kalimpong Region of Darjeeling Himalaya. *Environmental Monitoring and Assessment*, 194, p.234. https://doi.org/10.1007/s10661-022-09851-7

Devkota, K.C., Regmi, A.D., Pourghasemi, H.R., Yoshida, K., Pradhan, B., Ryu, I.C., Dhital, M.R. and Althuwaynee, O.F., 2013. Landslide susceptibility mapping using certainty factor, index of entropy, and logistic regression models in GIS and their comparison at Mugling-Narayanghat road section in Nepal Himalaya. *Natural Hazards*, 65(1), pp.135–165. https://doi.org/10.1007/s11069-012-0347-6

Feizizadeh, B., Roodposhti, M.S., Jankowski, P. and Blaschke, T., 2014. A GIS-based extended fuzzy multi-criteria evaluation for landslide susceptibility mapping. *Computers & Geosciences*, 73, pp.208–221. https://doi.org/10.1016/j.cageo.2013.11.009

Fell, R., Corominas, J., Bonnard, C., Cascini, L., Leroi, E. and Savage, W.Z., 2008. Guidelines for landslide susceptibility, hazard and risk zoning for land use planning. *Engineering Geology*, 102(3-4), pp.85–98. https://doi.org/10.1016/j.enggeo.2008.03.022

Fell, R., Whitt, G., Miner, A. and Flentje, P.N., 2007. Guidelines for landslide susceptibility, hazard and risk zoning for land use planning. *Australian Geomechanics Journal*, 42(1), pp.13–36

Gorsevski, P.V., Jankowski, P. and Gessler, P.E., 2006. A heuristic approach for mapping landslide hazard by integrating fuzzy logic with analytic hierarchy process. *Control and Cybernetics*, 35, pp.121–146.

Hadmoko, D.S., Lavigne, F. and Samodra, G., 2017. Application of a semiquantitative and GIS-based statistical model to landslide susceptibility zonation in Kayangan Catchment, Java, Indonesia. *Natural Hazards*, 87, pp.437–468. https://doi.org/10.1007/s11069-017-2772-z

Hemasinghe, H., Rangali, R.S.S., Deshapriya, N.L. and Samarakoon, L., 2018. Landslide susceptibility mapping using logistic regression model (a case study in Badulla District, Sri Lanka). *Procedia Engineering*, 212, pp.1046–1053. https://doi.org/10.1016/j.proeng.2018.01.135

Hoa, P.V., Tuan, N.Q., Hong, P.V., Thao, G.T.P. and Binh, N.A., 2023. GIS-based modeling of landslide susceptibility zonation by integrating the frequency ratio and objective–subjective weighting approach: a case study in a tropical monsoon climate region. *Frontiers in Environmental Science*, 11, p.1175567. https://doi.org/10.3389/fenvs.2023.1175567

Hong, Y., Adler, R. and Hufman, G., 2007. Use of satellite remote sensing data in the mapping of global landslide susceptibility. *Natural Hazards*, 43, pp.245–256. https://doi.org/10.1007/s11069-006-9104-z

Huan, Y., Song, L. and Khan, U., 2023. Stacking ensemble of machine learning methods for landslide susceptibility mapping in Zhangjiajie City, Hunan Province, China. *Environmental Earth Sciences*, 82, p.35. https://doi.org/10.1007/s12665-022-10723-z

Ilanloo, M., 2011. A comparative study of fuzzy logic approach for landslide susceptibility mapping using GIS: An experience of Karaj dam basin in Iran. *Procedia-Social and Behavioral Sciences*, 19, pp.668–676. https://doi.org/10.1016/j.sbspro.2011.05.184

Intergovernmental Panel on Climate Change (IPCC), 2021. *Climate Change 2021: The Physical Science Basis*. [online] Available at: https://wmo.int/media/magazine-article/regional-trends-extreme-events-ipcc-2021-report [Accessed 26 June 2024]

Jhunjhunwalla, M., Gupta, S.K. and Shukla, D.P., 2019. Landslide Susceptibility Zonation (LSZ) Using Machine Learning Approach for DEM Derived Continuous Dataset. In: Santosh, K. and Hegadi, R. (eds) *Communications in Computer and Information Science*, vol. 1037, Springer, p.45. https://doi.org/10.1007/978-981-13-9187-3_45

Kanungo, D.P., Sharma, S. and Pain, A., 2014. Artificial Neural Network (ANN) and Regression Tree (CART) applications for the indirect estimation of unsaturated soil shear strength parameters. *Frontiers of Earth Science*, 8, pp.439–456. https://doi.org/10.1007/s11707-014-0416-0

Kanwal, S., Atif, S. and Shafiq, M., 2016. GIS-based landslide susceptibility mapping of northern areas of Pakistan, a case study of Shigar and Shyok Basins. *Geomatics, Natural Hazards and Risk*. https://doi.org/10.1080/19475705.2016.1220023

Kirschbaum, D., Kapnick, S.B., Stanley, T. and Pascale, S., 2020. Changes in extreme precipitation and landslides over High Mountain Asia. *Geophysical Research Letters*, 47, e2019GL085347. https://doi.org/10.1029/2019GL085347

Kolat, C., Ulusay, R. and Suzen, M.L., 2012. Development of geotechnical micro zonation model for Yenisehir (Bursa, Turkey) located at a seismically active region. *Engineering Geology*, 127, pp.36–53. https://doi.org/10.1016/j.enggeo.2011.12.014

Kouli, M., Loupasakis, C. and Soupios, P., 2010. Landslide hazard zonation in high-risk areas of Rethymno Prefecture, Crete Island, Greece. *Natural Hazards*, 52, pp.599–621. https://doi.org/10.1007/s11069-009-9403-2

Lee, S., Choi, J. and Min, K., 2004. Probabilistic landslide hazard mapping using GIS and remote sensing data at Boun, Korea. *International Journal of Remote Sensing*, 25(11), pp.2037–2052. https://doi.org/10.1080/01431160310001618734

Lombardo, L., Tanyas, H. and Nicu, I.C., 2020. Spatial modeling of multi-hazard threat to cultural heritage sites. *Engineering Geology*, 277, p.105776. https://doi.org/10.1016/j.enggeo.2020.105776

Mahdadi, F., Boumezbeur, A., Hadji, R., et al., 2018. GIS-based landslide susceptibility assessment using statistical models: a case study from Souk Ahras province, N-E Algeria. *Arabian Journal of Geosciences*, 11, p.476. https://doi.org/10.1007/s12517-018-3770-5

Masson-Delmotte, V., Zhai, P., Pirani, A., Connors, S.L., Péan, C. and Berger, S., 2021. *Climate Change 2021: The Physical Science Basis*. Cambridge University Press https://dx.doi.org/10.1017/9781009157896

Merghadi, A., Yunus, A.P., Dou, J., Whiteley, J., Thai, Pham, B., Bui, D.T., Avtar, R. and Abderrahmane, B., 2020. Machine learning methods for landslide susceptibility studies: A comparative overview of algorithm performance. *Earth-Science Reviews*, 207, p.103225. https://doi.org/10.1016/j.earscirev.2020.103225

Othman, A.N., Naim, W.M. and Noraini, S., 2012. GIS-based multi-criteria decision making for landslide hazard zonation. *Procedia - Social and Behavioral Sciences*, 35, pp.595–602. https://doi.org/10.1016/j.sbspro.2012.02.126

Ozioko, O.H. and Igwe, O., 2020. GIS-based landslide susceptibility mapping using heuristic and bivariate statistical methods for Iva Valley and environs Southeast Nigeria. *Environmental Monitoring and Assessment*, 192, pp.1–19. https://doi.org/10.1007/s10661-019-7951-9

Pareta, K. and Pareta, U., 2015. Geomorphological interpretation through satellite imagery & DEM data. *American Journal of Geophysics Geochemistry Geosystems*, 1(2), pp.19–36.

Pareta, K., 2004. Hydro-geomorphology of Sagar district (MP): A study through remote sensing technique. In: Proceedings of XIX MP Young Scientist Congress, Madhya Pradesh Council of Science and Technology (MAPCOST), Bhopal.

Paulín, G.L., Bursik, M., Hubp, J.L., et al., 2014. A GIS method for landslide inventory and susceptibility mapping in the Río El Estado watershed, Pico de Orizaba volcano, Mexico. *Natural Hazards*, 71, pp.229–241. https://doi.org/10.1007/s11069-013-0911-8

Qazi, A., Singh, K. and Vishwakarma, D.K., 2023. GIS based landslide susceptibility zonation mapping using frequency ratio, information value, and weight of evidence: A case study in Kinnaur District HP, India. *Bulletin of Engineering Geology and the Environment*, 82, p.332. https://doi.org/10.1007/s10064-023-03344-8

Raju, M., 2002. Landslide hazard zonation for effective land management of mountainous terrain. In: *Arunachal Pradesh: Environmental Planning and Sustainable Development-Opportunities and Challenges*, Hepaticas Occasional Publication, (16), pp.439–443.

Saaty, T.L., 1980. *The Analytic Hierarchy Process*. McGrawhill, Juc. New York.

Saaty, T.L., 1990. How to make a decision: The analytic hierarchy process. *European Journal of Operational Research*, 48(1), pp.9–26. https://doi.org/10.1016/0377-2217(90)90057-I

Saravanan, S., Saranya, T., Abijith, D., Jacinth, J.J. and Singh, L., 2021. Delineation of groundwater potential zones for Arkavathi sub-watershed, Karnataka, India using remote sensing and GIS. *Environmental Challenges*, 5, p.100380. https://doi.org/10.1016/j.envc.2021.100380

Sarkar, S. and Kanungo, D.P., 2004. An integrated approach for landslide susceptibility mapping using remote sensing and GIS. *Photogrammetric Engineering & Remote Sensing*, 70(5), pp.617–625. http://dx.doi.org/10.14358/PERS.70.5.617

Shano, L., Raghuvanshi, T.K. and Meten, M., 2022. Landslide hazard zonation using logistic regression model: The case of Shafe and Baso catchments, Gamo Highland, Southern Ethiopia. *Geotechnique & Geology Engineering*, 40, pp.83–101. https://doi.org/10.1007/s10706-021-01873-1

Stanley, T. and Kirschbaum, D.B., 2017. A heuristic approach to global landslide susceptibility mapping. *Natural Hazards*, 87(1), pp.145–164. https://doi.org/10.1007/s11069-017-2757-y

Veerappan, R., Negi, A. and Siddan, A., 2017. Landslide susceptibility mapping and comparison using frequency ratio and analytical hierarchy process in part of NH-58, Uttarakhand, India. In: *Advancing Culture of Living with Landslides: Volume 2 Advances in Landslide Science* (pp. 1081–1091). Springer International Publishing. https://doi.org/10.1007/978-3-319-53498-5_123

Yadav, M., Pal, S.K., Singh, P.K. and Gupta, N., 2023. Landslide susceptibility zonation mapping using frequency ratio, information value model, and logistic regression model: A case study of Kohima District in Nagaland, India. In: Thambidurai, P. and Singh, T.N. (eds), *Landslides: Detection, Prediction, and Monitoring*. Springer, Cham. https://doi.org/10.1007/978-3-031-23859-8_17

Younes Cárdenas, N. and Erazo Mera, E., 2016. Landslide susceptibility analysis using remote sensing and GIS in the western Ecuadorian Andes. *Natural Hazards*, 81, pp.1829–1859. https://doi.org/10.1007/s11069-016-2157-8